

Supporting Information

A Ce/Ru co-doped SrFeO_{3-δ} Perovskite for a Coke-resistant Anode of a Symmetrical Solid Oxide Fuel Cell (SSOFC)

Bangxin Li,[†] Shuai He,[‡] Jibiao Li,^{§,||} Xiangling Yue,[‡] John T.S. Irvine,^{†,‡} Deti Xie,^{†,⊥} Jiupai Ni,^{*,†,⊥} and Chengsheng Ni^{*,†,⊥}

[†]*College of Resources and Environment, Southwest University, Chongqing 400716, China*

[‡]*School of Chemistry, University of St Andrews, Fife, KY16 9ST Scotland, UK*

[§]*Center for Materials and Energy (CME) and Chongqing Key Laboratory of Extraordinary Bond Engineering and Advanced Materials Technology (EBEAM), Yangtze Normal University, Chongqing 408100, China*

^{||}*Institute for Clean Energy and Advanced Materials, Southwest University, Chongqing 400715, China*

[⊥]*National Base of International S&T Collaboration on Water Environmental Monitoring and Simulation in Three Gorges Reservoir Region, Chongqing 400716 China*

Corresponding author: C.Ni.: nichengsheg@swu.edu.cn; J.Ni.: nijiupai@swu.edu.cn.

KEYWORDS: *ceria, propane, coke resistance, metal exsolution, oxide anode, carbonaceous fuel, catalysis, solid oxide fuel cell (SOFC).*

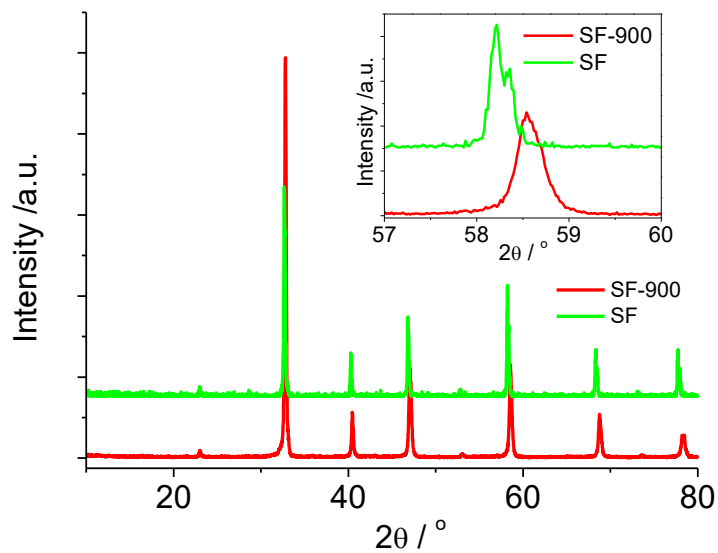


Figure S1. XRD patterns of SF at 1250 °C (SF) and 900 °C (SF-900), respectively. The inset shows magnifier part of the angle between 57° to 60°. The peak split in SF calcined at 1250 °C at 58.5° was an indication of non-cubic structure.

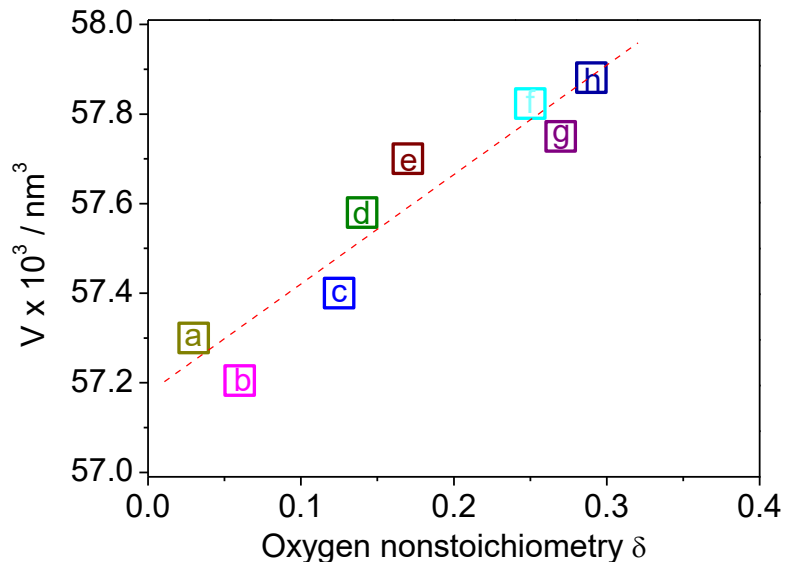


Figure S2. Pseudocubic cell volumes of SrFeO_3 according to the loss of oxygen content. The letters (a,¹ b,¹ c,² d,³ e,⁴ f,² g,³ and h⁵) represent the data sources. The dashed line is for visual assistance.

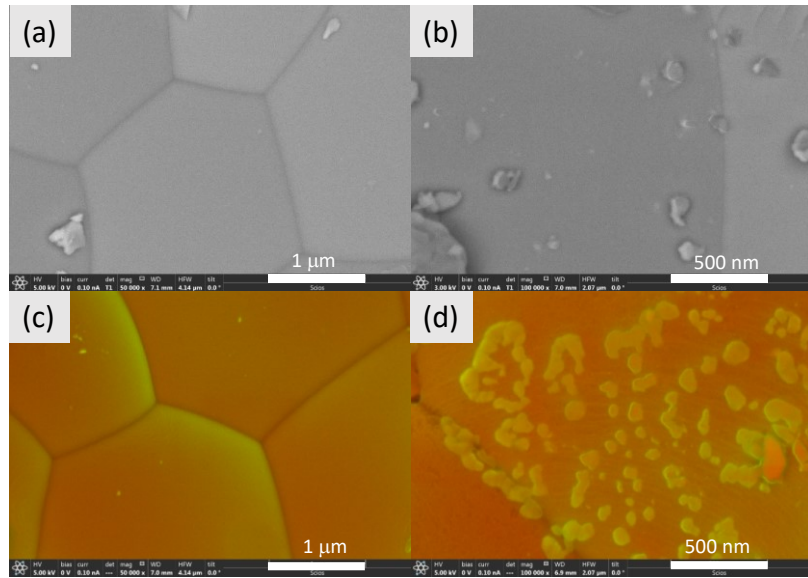


Figure S3. SEM of Ce20SF (a) before and (b) after reduction and Ce20SFR (c) before and (d) after reduction.

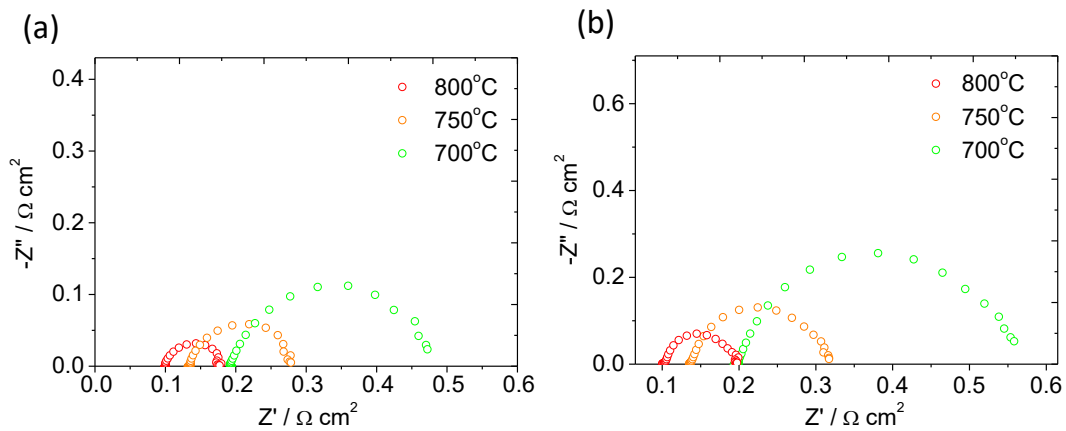


Figure S4. EIS of the half cell with (a) Ce20SF and (b) Ce20SFR electrode under ambient air.

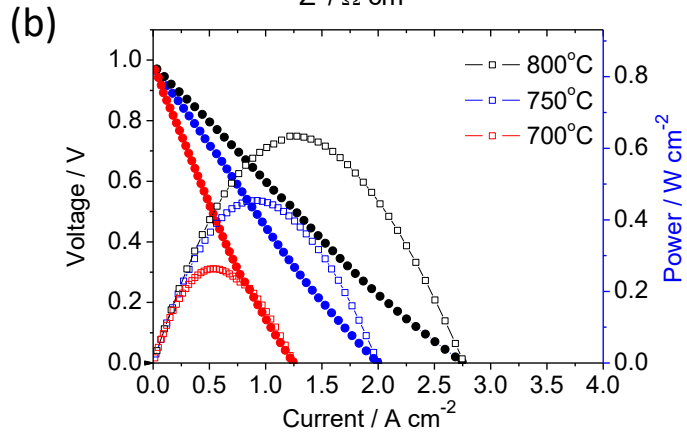
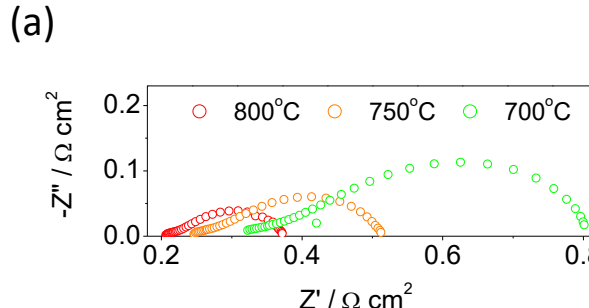


Figure S5. The EIS (a) and the IV and I-P curves (b) of Ce20SFR/LSGM/Ce20SFR with Pt slurry and wire as current collector using H₂ as fuel and air as oxidant. The straight-line plots (solid signals) correspond to the voltages (left y axis) and the curved plots (open signals) correspond to the power densities (right y axis). The thickness of the LSGM electrolyte is around 300 nm in thickness. The cell with Pt paste is calcined in air at 900 °C for 60 minutes before the fuel test.

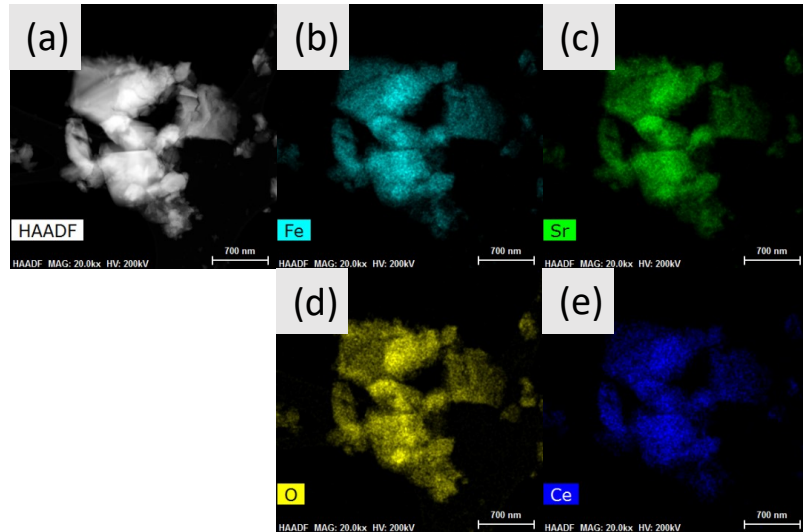


Figure S6. HAADF-STEM image (a) and EDX mapping (b, c, d, e) for individual Ce20SF reduced by H₂ for 5 hours.

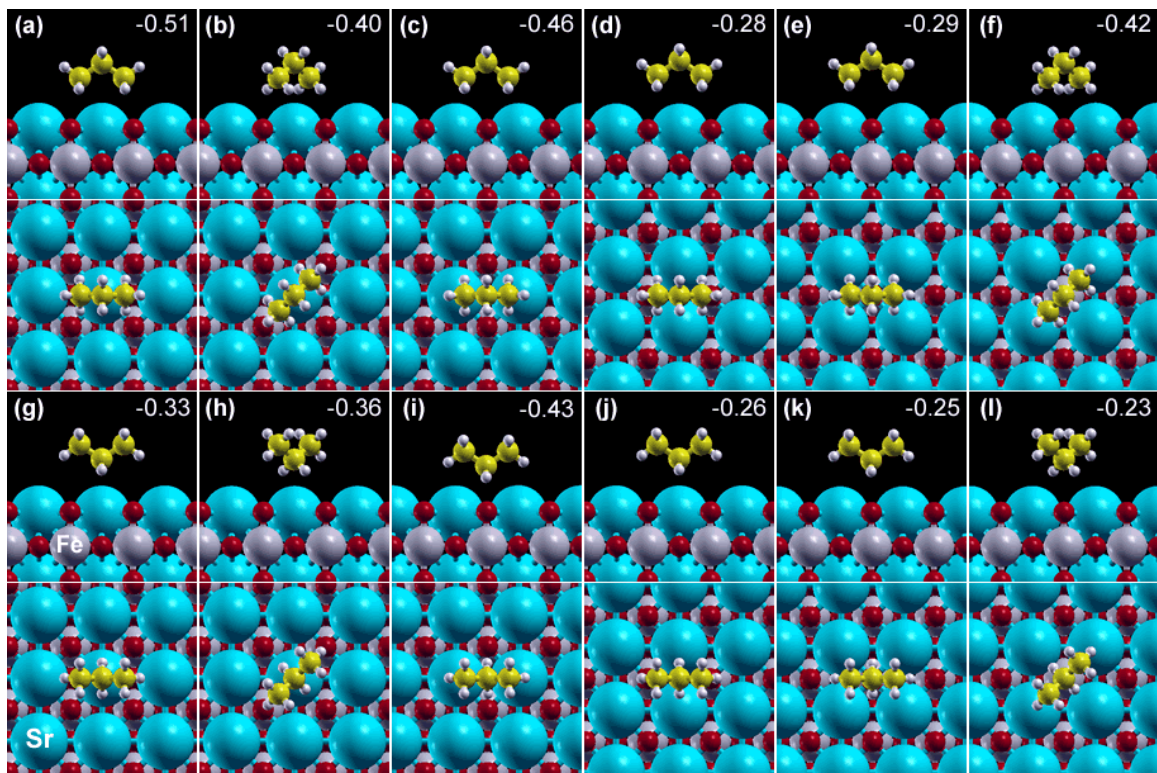


Figure S7. Site and orientation dependence of propane adsorbed on Ce doped SrFeO_3 (100). (a) top, (b) rotated at top, (c) bridge, (d) orthogonal bridge, (e) hollow, and (f) rotated at hollow. (g) to (l) are optimized structures of flipped propane. The adsorption energies by eV are given in the side views.

Table S1. Electrochemical performance of reported SSOFC with ferrite electrode.

Electrode	Electrolyte	R_p ($\Omega \text{ cm}^2$)	Peak power (mW cm^{-2})			Ref.
			H_2	H_2	Carbon hydrogen fuel	
$\text{La}_{0.6}\text{Sr}_{0.4}\text{Co}_{0.2}\text{Fe}_{0.7}\text{Mo}_{0.1}\text{O}_{3-\delta}$	LSGM (265 μm)	0.27	737 (800 °C)	400 (LPG)		⁶
$\text{Sr}_2\text{Fe}_{1.5}\text{Mo}_{0.5}\text{O}_{6-\delta}$	LSGM (275 μm)	0.26	835 (900 °C)	230 (CH_4)		⁷
$\text{Sr}_2\text{Fe}_{1.4}\text{Nb}_{0.1}\text{Mo}_{0.5}\text{O}_6$	LSGM (243 μm)	0.22	531 (800 °C)			⁸
$\text{Sr}_2\text{TiFe}_{0.9}\text{Mo}_{0.1}\text{O}_{6-\delta}$	LSGM (200 μm)	0.27	444 (800 °C)	300 (syngas containing H_2S)		⁹
$\text{Pr}_{0.4}\text{Sr}_{0.6}\text{Co}_{0.2}\text{Fe}_{0.7}\text{Nb}_{0.1}\text{O}_{3-\delta}$	LSGM (265 μm)	0.44	780 (850 °C)			¹⁰
$\text{La}_{0.8}\text{Sr}_{1.2}\text{Fe}_{0.9}\text{Co}_{0.1}\text{O}_{4\pm\delta}$	LSGM (1000 μm)	1.14	237 (800 °C)			¹¹
$\text{La}_{0.8}\text{Sr}_{0.2}\text{Fe}_{0.7}\text{Ni}_{0.3}\text{O}_{3-\delta}$	LSGM (350 μm)	0.10	540 (800 °C)			¹²
$\text{La}_{0.6}\text{Ce}_{0.1}\text{Sr}_{0.3}\text{Fe}_{0.9}\text{Ni}_{0.1}\text{O}_{3-\delta}$	LSGM (300 μm)	0.17	675 (800 °C)	210 (wet CH_4)		¹³
$\text{La}_{0.6}\text{Sr}_{0.4}\text{Co}_{0.2}\text{Fe}_{0.6}\text{Nb}_{0.2}\text{O}_{3-\delta}$	LSGM (200 μm)	0.59	400 (800 °C)	190 (CH_4)		¹⁴
$\text{La}_{0.5}\text{Sr}_{0.5}\text{Fe}_{0.9}\text{Nb}_{0.1}\text{O}_{3-\delta}$	LSGM (300 μm)	0.24	800 (800 °C)			¹⁵
$\text{La}_{0.3}\text{Sr}_{0.7}\text{Fe}_{1-x}\text{Cr}_x\text{O}_{3-\delta}$	LSGM (500 μm)	0.4	300 (800 °C)			¹⁶
$\text{Ce}_{0.2}\text{Sr}_{0.8}\text{Fe}_{0.95}\text{Ru}_{0.05}\text{O}_3$	LSGM (320 μm)	0.12	846 (800 °C)	310 (C_3H_8)		This work
$\text{Ce}_{0.2}\text{Sr}_{0.8}\text{FeO}_3$	LSGM (320 μm)	0.51	482 (800 °C)	190 (C_3H_8)		This work

Note: The temperature for carbonaceous fuel is the same as the one under H_2 fuel.

Reference

1. Blasco, J.; Stankiewicz, J.; Garcia, J., Phase segregation in the $Gd_{1-x}Sr_xFeO_{3-\delta}$ series. **2006**, Medium: X; Size: page(s) 898-908.
2. J.P, H.; S, S.; J.D, J.; X, X.; Dabrowski, B.; Mini, S.; C.W, K., Evolution of oxygen-vacancy ordered crystal structures in the perovskite series $Sr_nFe_nO_{3n-1}$ ($n=2, 4, 8$, and infinity), and the relationship to electronic and magnetic properties. *Journal of Solid State Chemistry* **2000**, *151*, 190-209.
3. Takeda, Y.; Kanno, R.; Takada, T.; Yamamoto, O.; Takano, M.; Bando, Y., Phase relation and oxygen-non-stoichiometry of Perovskite-like Compound $SrCoO_x$ ($2.29 < x > 2.80$). **1986**, *540* (9-10), 259-270.
4. Tsunekawa, S.; Imaeda, K.; Takei, H. J. M. R. B., Nonstoichiometry and superconductivity in $La_xMo_6S_y$. **1987**, *22* (5), 585-592.
5. Gibb; Terence, C. J. J. o. M. C., Reinterpretation of the magnetic structures of the perovskites $SrFeO_{2.710}$ and $Sr_2LaFe_3O_{8.417}$. **1994**, *4* (9), 1445-1449.
6. Lu, C.; Niu, B.; Yu, S.; Yi, W.; Luo, S.; Xu, B.; Ji, Y., Efficient and stable symmetrical electrode $La_{0.6}Sr_{0.4}Co_{0.2}Fe_{0.7}Mo_{0.1}O_{3-\delta}$ for direct hydrocarbon solid oxide fuel cells. *Electrochimica Acta* **2019**, *323*, 134857.
7. Liu, Q.; Dong, X.; Xiao, G.; Zhao, F.; Chen, F., A Novel Electrode Material for Symmetrical SOFCs. *Advanced Materials* **2010**, *22* (48), 5478-5482.
8. Gou, M.; Ren, R.; Sun, W.; Xu, C.; Meng, X.; Wang, Z.; Qiao, J.; Sun, K., Nb-doped $Sr_2Fe_{1.5}Mo_{0.5}O_{6-\delta}$ electrode with enhanced stability and electrochemical performance for symmetrical solid oxide fuel cells. *Ceramics International* **2019**, *45* (12), 15696-15704.
9. Niu, B.; Jin, F.; Zhang, L.; Shen, P.; He, T., Performance of double perovskite symmetrical electrode materials $Sr_2TiFe_{1-x}Mo_xO_{6-\delta}$ ($x = 0.1, 0.2$) for solid oxide fuel cells. *Electrochim. Acta* **2018**, *263*, 217-227.
10. Xie, Z.; Zhao, H.; Chen, T.; Zhou, X.; Du, Z., Synthesis and electrical properties of Al-doped $Sr_2MgMoO_{6-\delta}$ as an anode material for solid oxide fuel cells. *International Journal of Hydrogen Energy* **2011**, *36* (12), 7257-7264.
11. Lai, B.-K.; Kerman, K.; Ramanathan, S., Nanostructured $La_{0.6}Sr_{0.4}Co_{0.8}Fe_{0.2}O_3/Y_{0.08}Zr_{0.92}O_{1.96}/La_{0.6}Sr_{0.4}Co_{0.8}Fe_{0.2}O_3$ (LSCF/YSZ/LSCF) symmetric thin film solid oxide fuel cells. *Journal of Power Sources* **2011**, *196* (4), 1826-1832.
12. Ben Mya, O.; dos Santos-Gomez, L.; Porras-Vazquez, J. M.; Omari, M.; Ramos-Barrado, J. R.; Marrero-Lopez, D., $La_{1-x}Sr_xFe_{0.7}Ni_{0.3}O_{3-\delta}$ as both cathode and anode materials for Solid Oxide Fuel Cells. *International Journal of Hydrogen Energy* **2017**, *42* (36), 23160-23169.
13. Bian, L.; Duan, C.; Wang, L.; O'Hayre, R.; Cheng, J.; Chou, K.-C., Ce-doped $La_{0.7}Sr_{0.3}Fe_{0.9}Ni_{0.1}O_{3-\delta}$ as symmetrical electrodes for high performance direct hydrocarbon solid oxide fuel cells. *Journal of Materials Chemistry A* **2017**, *5* (29), 15253-15259.
14. Niu, B.; Jin, F.; Feng, T.; Zhang, L.; Zhang, Y.; He, T., A-site deficient ($La_{0.6}Sr_{0.4}$)(1-x) $Co_{0.2}Fe_{0.6}Nb_{0.2}O_{3-\delta}$ symmetrical electrode materials for solid oxide fuel cells. *Electrochimica Acta* **2018**, *270*, 174-182.
15. Bian, L.; Duan, C.; Wang, L.; Zhu, L.; O'Hayre, R.; Chou, K.-C., Electrochemical performance and stability of $La_{0.5}Sr_{0.5}Fe_{0.9}Nb_{0.1}O_{3-\delta}$ symmetric electrode for solid oxide fuel cells. *Journal of Power Sources* **2018**, *399*, 398-405.
16. Chen, M.; Paulson, S.; Thangadurai, V.; Birss, V., Sr-rich chromium ferrites as symmetrical solid oxide fuel cell electrodes. *Journal of Power Sources* **2013**, *236*, 68-79.